articles

molecular pharmaceutics

Induced Disorder in Protein–Ligand Complexes as a Drug-Design Strategy

Alejandro Crespo[†] and Ariel Fernández*[,†,‡]

Department of Bioengineering, Rice University, Houston, Texas 77005, Department of Experimental Therapeutics, M. D. Anderson Cancer Center—University of Texas, Houston, Texas 77030

Received November 20, 2007; Revised Manuscript Received January 7, 2008; Accepted January 13, 2008

Abstract: Protein associations are poorly understood from a chemical perspective. If the contrary were true, drug inhibitors would be routinely designed based on target structure. While enthalpy/entropy balance is critical for affinity optimization, most drug-design strategies focus solely on promoting favorable intermolecular interactions. However, protein−drug associations often entail an entropic penalty, mostly arising from induced fits, which compromises affinity. Rather than restricting the conformational freedom of the protein, this work reports on an alternative design strategy to enhance affinity by inducing conformational disorder. This approach is adopted to target kinases by boosting their conformational entropy, taking advantage of their structural plasticity. As proof of concept we redesigned the anticancer drug *imatinib* to inhibit the imatinib-resistant D816V mutant of the C-Kit kinase, one of imatinib's primary targets. The prototype is engineered to promote an entropic boost on the activation loop that restores affinity. We also show that induced disorder is actually operational in kinase inhibitory action: a comparison of the binding of imatinib and PD173955 to Bcr-Abl kinase reveals that imatinib forms stronger intermolecular nonbonded interactions than PD173955, yet the latter binds with higher affinity by boosting the complex entropy. Induced disorder thus becomes a promising concept for drug design.

Keywords: Protein−drug affinity; kinase inhibitor; entropic penalty; induced disorder; conformational entropy; Bcr-Abl kinase; C-Kit kinase; imatinib; PD173955

Introduction

Drug discovery remains essentially a serendipitous endeavor, mainly because we do not fully comprehend the physical basis of ligand-target affinity.[1–3] Unlike the historical method of trial-and-error, rational drug design is based on the knowledge of the three-dimensional structure and the specific chemical response of the target.[4] Thus, rational design is typically geared at fostering and optimizing intermolecular nonbonding interactions between the lead compound and the target.[5–8] However, protein–ligand associations often entail an entropic penalty that compromises

* Corresponding author. Mailing address: Department of Bioengineering, Rice University, Houston, TX 77005. Phone: (713)348-3681. Fax: (713)348-3699. E-mail: arifer@rice.edu.

† Rice University.

‡ Anderson Cancer Center—University of Texas.

(1) Liddington, R. C. Structural basis of protein-protein interactions. *Methods Mol. Biol.* **2004**, *261*, 3–14.

(2) Fernández, A.; Scheraga, H. A. Insufficiently dehydrated hydrogen bonds as determinants of protein interactions. *Proc. Natl. Acad. Sci. USA* **2003**, *100*, 113–118.

(3) Fuxreiter, M.; Simon, I.; Friedrich, P.; Tompa, P. Preformed structural elements feature in partner recognition by intrinsically unstructured proteins. *J. Mol. Biol.* **2004**, *338*, 1015–1026.

(4) Whitesides, G. M.; Krishnamurthy, V. M. Designing ligands to bind proteins. *Q. Rev. Biophys.* **2005**, *38*, 385–395.

(5) Freire, E. A thermodynamic guide to affinity optimization of drug candidates. In *Proteomics and protein-protein interactions: Biology, chemistry, bioinformatics, and drug design*; Waksman, G., Ed.; Protein Reviews 3; Springer: New York, 2005; pp 291–307..

(6) Gohlke, H.; Klebe, G. Approaches to the description and prediction of the binding affinity of small-molecule ligands to macromolecular receptors. *Angew. Chem., Int. Ed.* **2002**, *41*, 2644–2676.

10.1021/mp700148h CCC: $40.75
Published on Web 02/16/2008

affinity. This cost typically arises from induced fits in the target protein and motional constraints on the ligand.[4,9,10]

Rather than restricting the conformational space of the protein, we propose and validate the alternative strategy to enhance ligand affinity by inducing and controlling conformational *disorder* in the protein target upon complexation. Protein kinases are ideal binding partners to explore this possibility, since their folds include flexible loops framing the ligand binding site, i.e. the ATP pocket.[11] Furthermore, kinases have been successfully targeted in molecular cancer therapy.[12,13]

This approach is inspired by a comparison of the binding of two drug ligands, imatinib[7] (Gleevec, STI-571) and PD173955,[14] to the Bcr-Abl kinase. This protein is a constitutively active chimera resulting from chromosomal translocation and has been identified as a major target to treat chronic myeloid leukemia.[15] Imatinib binds to Bcr-Abl in the nanomolar range (K_d = 37 nM),[7] burying 1251 Å^2 of surface area.[14] It makes six intermolecular hydrogen bonds (Figure 1), and the majority of contacts are mediated by van der Waals interactions with residues F317, V256, A269, K271, I313, V299, R362, V289, A380, M290, F382, Y253, L248, L370 and G321.[14] Instead, the smaller PD173955 compound (913 Å^2 of buried surface area) forms only two intermolecular hydrogen bonds (Figure 2) and forms fewer van der Waals contacts (engaging residues G321, V256,

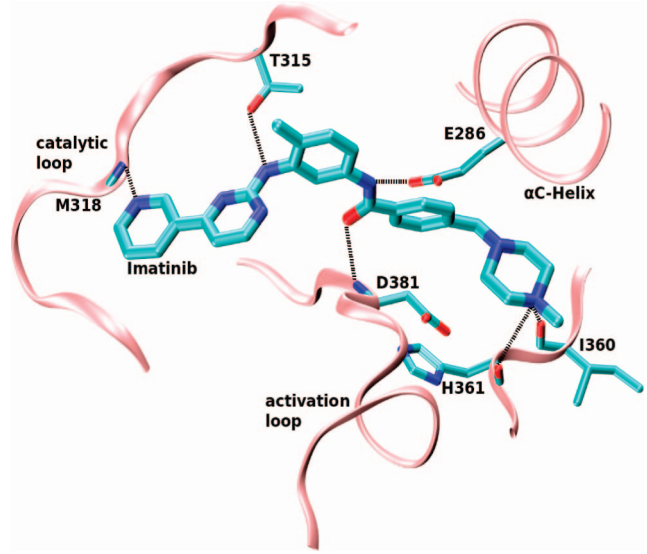

Figure 1. Intermolecular hydrogen bonds (dashed lines) at the ATP-binding site of Bcr-Abl kinase (PDB 1IEP) in the induced-fit inactive conformation generated upon complexation with imatinib.

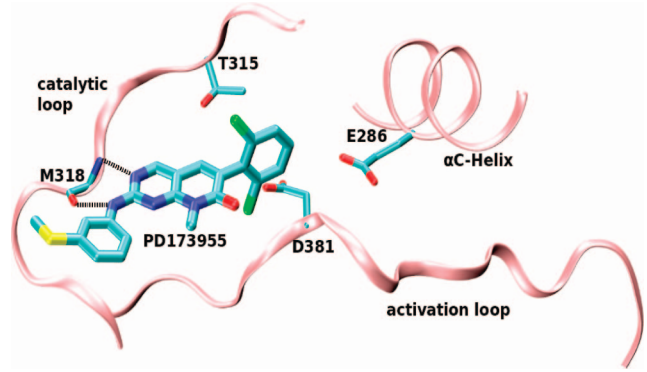

Figure 2. Intermolecular hydrogen bonds (dashed lines) at the ATP-binding site of Bcr-Abl kinase (PDB 1M52) in the induced-fit active conformation generated upon complexation with PD173955.

Y253, K272, M290, I313, T315, L370, Q269, T319), *yet it has higher affinity*: K_d = 5 nM.[14] Strikingly, two chlorine atoms in the terminal ring of PD173955 are positioned in the complex in proximity to nonpolar residues in floppy regions: V299, L370, F382 in the activation loop, V256 in the P-loop and I313 in the catalytic loop (Figure 3). Hence, besides the scarcity of favorable intermolecular interactions, there are polar–hydrophobic mismatches in the PD173955 complex.

These observations prompt us to enquire about the driving factor for the higher affinity of PD173955. The higher affinity is likely due to a larger sampling of the conformational space of the protein in the complex when compared with the uncomplexed protein. The polar−hydrophobic mismatches in the complex, together with the location of the hydrophobes in floppy regions (Figure 3), suggest an entropy-driven association realizing a *disorder-upon-binding* transition: The clustering nonpolar residues hinders chlorine hydration, and

(7) Schindler, T.; Bornmann, W. G.; Pellicena, P.; Miller, W. T.; Clarkson, B.; Kuriyan, J. Structural Mechanism for STI-571 Inhibition of Abelson Tyrosine Kinase. *Science* **2000**, *289*, 1938–1942.
(8) Garcia-Viloca, M.; Gao, J.; Karplus, M.; Truhlar, D. G. How enzymes work: Analysis by modern rate theory and computer simulations. *Science* **2004**, *303*, 186–195.
(9) Chang, C. A.; Chen, W.; Gilson, M. K. Ligand configurational entropy and protein binding. *Proc. Natl. Acad. Sci. USA* **2007**, *104*, 1534–1539.
(10) Frederick, K. K.; Marlow, M. S.; Valentine, K. G.; Wand, A. J. Conformational entropy in molecular recognition by proteins. *Nature* **2007**, *448*, 325–330.
(11) Huse, M.; Kuriyan, J. The conformational plasticity of protein kinases. *Cell* **2002**, *109*, 275–282.
(12) Schittenhelm, M. M.; Shiraga, S.; Schroeder, A.; Corbin, A. S.; Griffith, D.; Lee, F. Y.; Bokemeyer, C.; Deininger, M. W. N.; Druker, B. J.; Heinrich, M. C. Dasatinib (BMS-354825), a dual SRC/ABL kinase inhibitor, inhibits the kinase activity of wild-type, juxtamembrane, and activation loop mutant KIT isoforms associated with human malignancies. *Cancer Res.* **2006**, *66*, 473–481.
(13) Shah, N. P.; Lee, F. Y.; Luo, R.; Jiang, Y.; Donker, M.; Akin, C. Dasatinib (BMS-354825) inhibits KIT^{D816V}, an imatinib-resistant activating mutation that triggers neoplastic growth in most patients with systemic mastocytosis. *Blood* **2006**, *108*, 286–291.
(14) Nagar, B.; Bornmann, W. G.; Pellicena, P.; Schinlder, T.; Veach, D. R.; Miller, W. T.; Clarkson, B.; Kuriyan, J. Crystal structures of the kinase domain of c-Abl in complex with the small molecule inhibitors PD173955 and Imatinib (STI-571). *Cancer Res.* **2002**, *62*, 4236–4243.
(15) Donato, N. J.; Talpaz, M. Clinical use of tyrosine kinase inhibitors: Therapy for chronic myelogenous leukemia and other cancers. *Clin. Cancer Res.* **2000**, *6*, 2965–2966.

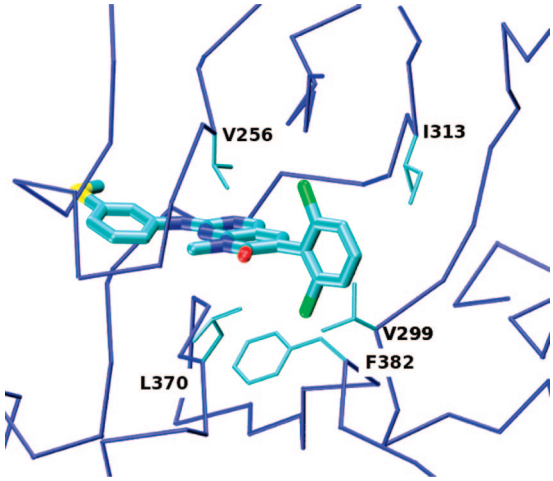

Figure 3. Hydrophobic−polar mismatches in the complexation of Bcr-Abl with PD173955. The chlorine atoms in the ligand are shown in green. Hydrophobic residues with nonpolar groups within spheres of radius 4.8 Å (~thickness of three water layers) centered at the chlorine atoms are labeled, and their side chains are displayed (cyan).

hence the loopy regions containing the hydrophobes boost their conformational exploration to enable the hydration of the chlorines. These inferences are validated by our thermodynamic computations of the ligand−target complexation presented below.

This paradox and its resolution point to the possibility of designing entropy-boosting ligands, an approach validated in this work. As proof of concept, we show how to redesign imatinib, turning the drug into an entropy enhancer to overcome imatinib resistance arising in a major imatinib target through somatic mutation. Imatinib binds the C-Kit kinase,[16] a target for treating gastrointestinal stromal tumors (GISTs).[17] However, after extensive drug treatment, this kinase develops the D816V-mutation in the activation loop[18,19] which confers resistance to the drug,[12,13] while still maintaining its functionality. The decrease in imatinib affinity toward the D816V mutant was proven to be mainly due to an enhancement in conformational entropy of the imatinib-resistant unbound kinase, entailing an increased entropic penalty upon drug association.[20]

In light of this fact and contrary to established design principles,[5–8] our prototype involves modifying imatinib to promote an *unfavorable* interaction with the activation loop of the kinase, hence increasing the entropy of the complex. Molecular dynamics simulations provide thermodynamic and structural guidance to the design, revealing an increase in the binding affinity of the entropy-boosting prototype toward the mutant when compared with imatinib. *In vitro* kinetic assays of downstream phosphorylation activity show a *dual* inhibitory impact of the prototype against *both* wild-type and imatinib-resistant kinase. The selective yet dual inhibitory activity of our prototype is corroborated *in vitro* using a high-throughput bacteriophage-display kinase screening[21] covering a large fraction of the human kinome. Finally, the activity of the entropy-boosting molecule against the drug-resistant variant is contrasted with the lack of efficacy of imatinib by performing Western blot assays on cell lines that express the imatinib D816V resistant mutant.

Materials and Methods

Molecular Dynamics/Free-Energy Calculations. Classical molecular dynamics (MD) simulations were performed starting from the crystal structure of the corresponding kinase−ligand complex: Bcr-Abl with imatinib (PDB 1IEP),[14] Bcr-Abl with PD173955 (PDB 1M52),[14] C-Kit with imatinib (PDB 1T46).[16] In the latter case, simulations were performed for the wild-type kinase and for the *in silico* generated D816V mutant complexed with both imatinib and the prototype. To describe the induced fit, we performed simulations of the uncomplexed forms of the kinases and of the isolated ligands. For control purposes, additional simulations were performed adopting a modified PD173955 compound, where two hydrogen atoms replaced the chlorine atoms. All simulations were performed using the Amber9 package.[22–25] Details of the simulations are provided in the Supporting Information.

(16) Mol, C. D.; Dougan, D. R.; Schneider, T. R.; Skene, R. J.; Kraus, M. L.; Scheibe, D. N.; Snell, G. P.; Zou, H.; Sang, B.; Wilson, K. P. Structural basis for the autoinhibition and STI-571 inhibition of c-Kit tyrosine kinase. *J. Biol. Chem.* **2004**, *279*, 31655–31663.

(17) Attoub, S.; Rivat, C.; Rodrigues, S.; Van Bocxlaer, S.; Bedin, M.; Bruyneel, E.; Louvet, C.; Kornprobst, M.; Andre, T.; Mareel, M.; Mester, J.; Gespach, C. The c-kit tyrosine kinase inhibitor STI571 for colorectal cancer therapy. *Cancer Res.* **2002**, *62*, 4879–4883.

(18) Furitsu, T.; Tsujimura, T.; Tono, T.; Ikeda, H.; Kitayama, H.; Koshimizu, U.; Sugahara, H.; Butterfield, J. H.; Ashman, L. K.; Kanayama, Y.; Matsuzawa, Y.; Kitamura, Y.; Kanakura, Y. Identification of mutations in the coding sequence of the proto-oncogene c-kit in a human mast cell leukemia cell line causing ligand-independent activation of c-kit product. *J. Clin. Invest.* **1993**, *92*, 1736–1744.

(19) Nagata, H.; Worobec, A. S.; Oh, C. K.; Chowdhury, B. A.; Tannenbaum, S.; Suzuki, Y.; Metcalfe, D. D. Identification of a point mutation in the catalytic domain of the protooncogene c-kit in peripheral blood mononuclear cells of patients who have mastocytosis with an associated hematologic disorder. *Proc. Natl. Acad. Sci. USA* **1995**, *92*, 10560–10564.

(20) Fernández, A.; Sanguino, A.; Peng, Z.; Crespo, A.; Ozturk, E.; Zhang, X.; Wang, S.; Bornmann, W.; Lopez-Berestein, G. Rational drug redesign to overcome drug resistance in cancer therapy: imatinib moving target. *Cancer Res.* **2007**, *67*, 4028–4033.

(21) Fabian, M. A.; Biggs, W. A.; Treiber, D. K.; Atteridge, C. E.; Azimioara, M. D.; Benedetti, M. G.; Carter, T.; Ciceri, P.; Edeen, P. T.; Floyd, M.; Ford, J. M.; Galvin, M.; Gerlach, J. L.; Grotzfeld, R. M.; Herrgand, S.; Insko, D. E.; Insko, M. A.; Lai, A.; Lélias, J. M.; Mehta, S.; Milanov, Z. V.; Velasco, A. M.; Wodicka, L. M.; Patel, H. K.; Zirrankar, P. P.; Lockhart, D. A. A small molecule-kinase interaction map for clinical kinase inhibitors. *Nat. Biotechnol.* **2005**, *23*, 329–336.

The free energies of binding for the different kinase−ligand complexes were calculated using the MMGBSA method.[26–28] In this method free energies are calculated for snapshot structures taken from the MD trajectory. The average binding free energy (ΔG_{bind}) is calculated as the sum of the energetic contributions, which correspond to the average molecular mechanical gas-phase energies ($E_{MM} = E_{elec} + E_{vdW}$) and the average solvation free energies (ΔG_{solv}), plus the entropic contributions ($-T\Delta S$). The molecular mechanical energies were evaluated in a single MD step using an infinite cutoff for nonbonded interactions. In order to mask the hydrogen-bond contributions, the partial charges of the ligand atoms involved in such interactions were set at zero value and added to their first neighbor atoms to conserve the total charge of the molecules. The solvation free energies were estimated as the sum of an electrostatic solvation energy, calculated with the generalized Born model,[29] plus a nonpolar solvation energy, proportional to the solvent-accessible surface area, which includes the entropy cost of creating a solute-sized cavity in the solvent.[26] Finally, the entropic contributions were estimated by calculating the quasiharmonic entropy,[30–32] in which the atomic fluctuation matrix is calculated as the mass-weighted covariance matrix obtained from the snapshots of the MD simulation (Supporting Information).

Synthesis of Imatinib Derivative Prototype. The synthesis of the imatinib derivative resulting by adding a chlorine atom at position 6 on the pyperidine ring recapitulates Novartis patent WO 03027100A1, 2003,[33] replacing the *N*,*N*-dimethylformamide dimethyl acetal for *N*,*N*-dimethylformamide chloro-dimethyl acetal in the first step of synthesis. The total synthesis and spectroscopic characterization of the prototype is provided as Supporting Information.

Spectrophotometric Kinetic Assay. The inhibitory efficacy of the prototype was tested by measuring the rate of downstream phosphorylation of active wild-type C-Kit kinase and active variant D816V (Upstate, Millipore) in the presence of inhibitors. The spectrophotometric assay adopted couples ADP production with NADH oxidation, determined by absorbance reduction at 340 nm, as described in ref 7. Details are provided in the Supporting Information.

High-Throughput Screening. A high-throughput screening of the prototype inhibitor at 10 μM was conducted by Ambit Biosciences (San Diego, CA) against a bacteriophage library displaying 240 human kinases, using imatinib screening as control.[21] A rough estimation of the binding constant (K_d^{-1}) for each assay was provided by the single-hit value in the primary screen at a single compound concentration. Kinase profiling was performed using a bacteriophage library displaying fused human kinases that may attach at the ATP site to a fixed-ligand matrix which may be competitively displaced from binding by the tested compound.[21]

Western Blots. Murine pro-B cells Ba/F3 (ATCC, Manassas, VA) expressing C-Kit D816V mutation[34] were incubated untreated and treated with imatinib or prototype inhibitor (0.1, 1 and 10 μM) for 12 hs. After treatment, cell pellets were lysed, and protein mixtures were separated through gel electrophoresis (SDS−PAGE). Membranes were subsequently probed with specific antibodies. Details are provided in the Supporting Information.

(22) Case, D. A.; Darden, T. A.; Cheatham, T. E., III; Simmerling, C. L.; Wang, J.; Duke, R. E.; Luo, R.; Merz, K. M., Jr.; Pearlman, D. A.; Crowley, M.; Walker, R. C.; Zhang, W.; Wang, B.; Hayik, S.; Roitberg, A. E.; Seabra, G.; Wong, K. F.; Paesani, F.; Wu, X.; Brozell, S.; Tsui, V.; Gohlke, H.; Yang, L.; Tan, C.; Mongan, J.; Hornak, V.; Cui, G.; Beroza, P.; Mathews, D. H.; Schafmeister, C.; Ross W. S.; Kollman, P. A. *AMBER 9*; University of California: San Francisco, 2006.

(23) Pearlman, D. A.; Case, D. A.; Caldwell, J. W.; Ross, W. S.; Cheatham, T. E., III; DeBolt, S.; Ferguson, D.; Seibel, G.; Kollman, P. A. AMBER, a package of computer programs for applying molecular mechanics, normal mode analysis, molecular dynamics and free energy calculations to simulate the structural and energetic properties of molecules. *Comput. Phys. Commun.* **1995**, *91*, 1–41.

(24) Case, D. A.; Cheatham, T. E., III; Darden, T. A.; Gohlke, H.; Luo, R.; Merz, K. M., Jr.; Onufriev, A.; Simmerling, C. L.; Wang, B.; Woods, R. The Amber biomolecular simulation programs. *J. Comput. Chem.* **2005**, *26*, 1668–1688.

(25) Cornell, W. D.; Cieplak, P.; Bayly, C. I.; Gould, I. R., Jr.; Ferguson, D.; Pellmeyer, D. C.; Fox, T.; Cadwell, J. W.; Kollman, P. A. A second generation force-field for the simulation of proteins, nucleic-acids, and organic-molecules. *J. Am. Chem. Soc.* **1995**, *117*, 5179–5197.

(26) Lee, M. R.; Duan, Y.; Kollman, P. A. Use of MM-PB-SA in estimating the free energies of proteins: Application to native, intermediates, and unfolded villin headpiece. *Proteins: Struct., Funct., Genet.* **2000**, *39*, 309–316.

(27) Wang, J.; Morin, P.; Wang, W.; Kollman, P. A. Use of MM-PBSA in reproducing the binding free energies to HIV-1 RT of TIBO derivatives and predicting the binding mode to HIV-1 RT of Efavirenz by docking and MM-PBSA. *J. Am. Chem. Soc.* **2001**, *123*, 5221–5230.

(28) Swanson, J. M. J.; Henchman, R. H.; McCammon, J. A. Revisiting free energy calculations: A theoretical connection to MM/PBSA and direct calculation of the association free energy. *Biophys. J.* **2004**, *86*, 67–74.

(29) Still, W. C.; Tempczyk, A.; Hawley, R. C.; Hendrickson, T. Semianalytical treatment of solvation for molecular mechanics and dynamics. *J. Am. Chem. Soc.* **1990**, *112*, 6127–6129.

(30) Andricioaei, I.; Karplus, M. On the calculation of entropy from covariance matrices of the atomic fluctuations. *J. Chem. Phys.* **2001**, *115*, 6289–6292.

(31) Surjit, B.; Andrews, D. Q.; Beveridge, D. L. Induced fit and the entropy of structural adaptation in the complexation of CAP and l-repressor with cognate DNA sequences. *Biophys. J.* **2005**, *88*, 3147–3157.

(32) Harris, S. A.; Gavathiotis, E.; Searle, M. S.; Orozco, M.; Laughton, C. A. Coperativity in drug-DNA recognition: A molecular dynamics study. *J. Am. Chem. Soc.* **2001**, *123*, 12658–12663.

(33) Li, J. J.; Johnson, D. S.; Sliskovic, D. R.; Roth, B. D. *Contemporary drug synthesis*; Wiley-Interscience: Hoboken, NJ, 2004; pp 32–33..

(34) Corbin, A. S.; Griswold, I. J.; La Rosée, P.; Yee, K. W. H.; Heinrich, M. C.; Reimer, C. L.; Druker, B. J.; Deininger, M. W. N. Sensitivity of oncogenic KIT mutants to the kinase inhibitors MLN518 and PD180970. *Blood* **2004**, *104*, 3754–3757.

Results and Discussion

The entropy-boost concept was first validated by showing that the difference in binding affinity between imatinib[7] and PD173955[14] against Bcr-Abl is mainly due to the induced disorder promoted upon association with the latter. Our calculated binding free energies (ΔG_{bind}) are −19.1 and −22.5 kcal/mol, for Bcr-Abl complexed with imatinib and PD173955, respectively, confirming the experimental higher affinity of the latter.[14] The energetic contributions are −68.45 and −54.27 kcal/mol, respectively, consistent with stronger electrostatic and van der Waals interactions between imatinib and Bcr-Abl in comparison with PD173955 ($\Delta E_{elec} = -30$ and −19 kcal/mol; $\Delta E_{vdW} = -72$ and −55 kcal/mol; for imatinib and PD173955, respectively). In both complexes, all hydrogen bonds are stable throughout the simulations, with average H−X (X = N or O) distances smaller than 2.3 Å and average X−H−X′ (X, X′ = N or O) angles larger than 145°, indicating similar hydrogen-bond strengths. Moreover, the effect of masking the hydrogen-bond interactions (Materials and Methods) results in a decrease of the energetic contributions to −56.41 (−12) and −47.07 (−7) kcal/mol, for imatinib and PD173955, respectively ($\Delta\Delta E_{elec} = -29$ and −12 kcal/mol, respectively). This suggests a stronger hydrogen-bond contribution for imatinib binding when contrasted with PD173955 binding, consistent with the larger number of intermolecular hydrogen bonds formed in the former kinase−ligand complex.

On the other hand, our computed entropic contributions ($-T\Delta S$) are 49.33 and 31.80 kcal/mol, for imatinib and PD173955, respectively. Thus, the reason for the higher affinity of PD173955 is the reduction of the entropic penalty ($T\Delta S \sim 17$ kcal/mol) that translates into a larger sampling of the conformational space of the protein within the complex (3629 eu) when compared with imatinib (3580 eu). The polar−hydrophobic mismatches of the complex, combined with the location of the hydrophobes within flexible regions (Figure 3), enable the induced disorder mode of association of PD173955. The estimated errors of the calculated quasi-harmonic entropies (Supporting Information) for all systems are ∼3 eu (0.08%) or 1.5RT (0.9 kcal/mol, for T = 300 K). Thus, the entropy differences reported in this work (15 kcal/mol in this case, ≥5 kcal/mol in general, for T = 300 K) are significant. Our parameters and results are consistent with previously reported calculations.[26,27,31,32]

Moreover, replacing the two chlorine atoms in PD173955 by hydrogen atoms drastically decreases the binding free energy (ΔG_{bind}) to −8.7 kcal/mol. The energetic contribution decreases to −44.58 kcal/mol, consistent with the lack of van der Waals interactions between the chlorine atoms and the hydrophobic core of the kinase. However, our computed entropic contribution ($-T\Delta S$) increases to 35.85 kcal/mol, consistent with a reduction of the entropy content of the complex (3606 eu) when compared with the original PD173955 compound (3629 eu). These computations reveal that the ligand chlorine atoms are essential to increase the binding affinity by inducing disorder upon association.

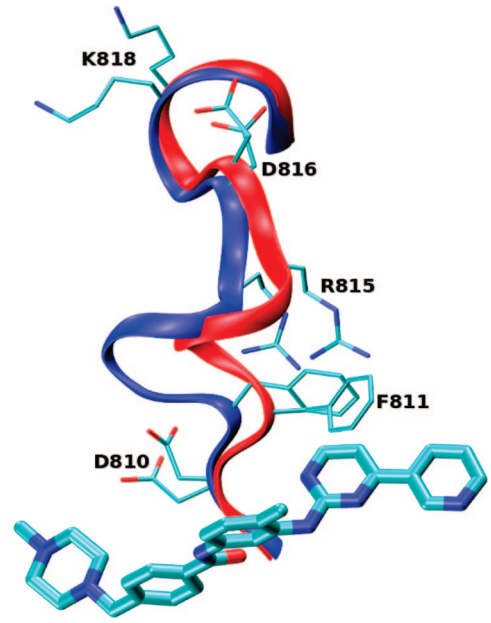

Figure 4. Location of imatinib relative to the activation loop (ribbon representation) of C-Kit kinase within the ligand-kinase complex PDB 1T46 (blue). The superimposed autoinhibited conformation (PDB 1T45, red) shows the induced-fit generated in the activation loop by the drug. Relevant residues are depicted for clarity.

As proof of concept validating the design strategy of association-inducing disorder, we now show how to re-engineer imatinib, turning it into an entropy booster to overcome imatinib resistance in the C-Kit kinase. Imatinib promotes an induced fit in the activation loop of the wild-type kinase. This structural adaptation readjusts the conserved catalytic DFG motif to avoid a steric clash with the side chain of F811 (PDB 1T46, imatinib complex; PDB 1T45, autoinhibited; Figure 4).[16] It has been reported that the deleterious effects of D816V mutation may derive from the ability of D816 to stabilize a small positively charged α-helical dipole by virtue of its negative charge.[16] D816 serves as the amino-terminal capping residue for approximately one turn of α-helix including residues I817, K818, N819, D820. Hence, a mutation of D816 to a hydrophobic residue (V816) is likely to destabilize the helical segment. Moreover, the drug-resistant effect of the D816V mutant may be caused by an inversion of the conformation of the activation loop such that the side chain of V816 points inward, flipping the side chain of R815 from its autoinhibited position (directed toward D810), destabilizing imatinib binding.[16]

We previously reported the free energies of binding of imatinib to both the wild-type and D816V mutant C-Kit kinases.[20] Our calculated binding free energies (ΔG_{bind}) are −17.0 and −4.5 kcal/mol, for wild-type and D816V complexation with imatinib, respectively. The energetic contributions are −57.69 and −59.15 kcal/mol, and the entropic contributions ($-T\Delta S$) 40.70 and 54.69 kcal/mol, respectively, suggesting that the decrease in imatinib affinity is mainly due to entropic effects. The structure and dynamics of imatinib complexed with wild-type and D816V obtained after

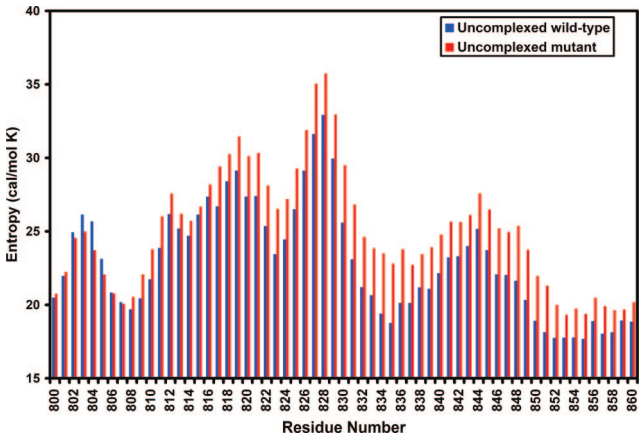

Figure 5. Entropic contributions (cal/mol K, 1 cal/mol *K* = 1 eu) as a function of the C-Kit residue number in the activation loop (residues 804 to 837) for uncomplexed free forms of C-Kit kinase: wild-type (blue) and D816V mutant (red).

the MD simulations are very similar. They both resemble the original structure (PDB 1T46) and have the same entropy content (3537 and 3540 eu, respectively). However, differences arise in the uncomplexed forms: the wild-type uncomplexed structure adopted is similar to the autoinhibited structure (PDB 1T45), with a salt-bridge between D816 and K818 that stabilizes the α-helix in the activation loop. In the D816V uncomplexed mutant this salt-bridge is absent, and the hydrophilic to hydrophobic destabilizing amino acid substitution in the solvent-exposed activation loop increases its entropy content, resulting in the side chain of V816 pointing inward with consequent formation of the D810−R815 salt-bridge. Thus, *imatinib resistance arises from the entropy increase* ($T\Delta S \sim 14$ kcal/mol) *of the uncomplexed mutant with respect to the uncomplexed wild-type* (Figure 5; entropy contributions 3503 and 3453 eu, respectively).

To validate our entropy-boosting design strategy and generate a drug that competitively inhibits the D816V mutant, we re-engineer imatinib to increase the entropy content of the complex. Thus, our molecular prototype involves the incorporation of a chlorine atom at position 6 in the pyrimidine ring of imatinib[33] pointing toward the F811 residue of the activation loop of the kinase (Figure 6), thus promoting a polar–hydrophobic mismatch. The introduction of a bulky chlorine atom bearing negative charge density will destabilize the aromatic F811 residue located in such a floppy region, increasing the conformational flexibility of the loop. The computed binding free energy (ΔG_{bind}) of our prototype with the D816V mutant is −14.9 kcal/mol, with energetic and entropic ($-T\Delta S$) contributions of −60.17 and 45.29 kcal/mol, respectively. Thus, *the prototype restores the affinity for the mutant by promoting an entropic boost on the activation loop, hence increasing the complex entropy content* ($T\Delta S \sim 10$ kcal/mol) *with respect to the imatinib mutant counterpart* (Figure 7, 3582 and 3540 eu, respectively). This effect accounts for the difference in binding affinity.

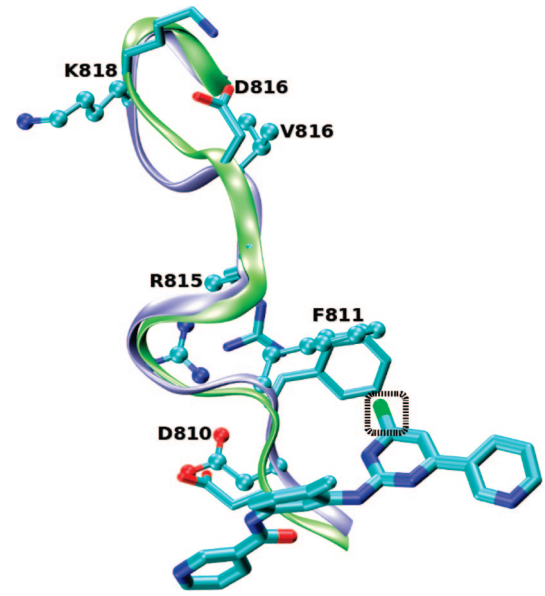

Figure 6. Location of entropy-boosting prototype inhibitor relative to the activation loop of D816V mutant (ribbon representation, ice blue) and wild-type (ribbon representation, lime) kinases in conformations generated by MD simulations. There is an increase in loop flexibility produced by the prototype as it promotes the displacement of hydrophobic residue F811 in the kinase. The appended chlorine atom is depicted in green (black box). Relevant residues are depicted for clarity (wild-type, licorice motif; mutant, balls and sticks motif).

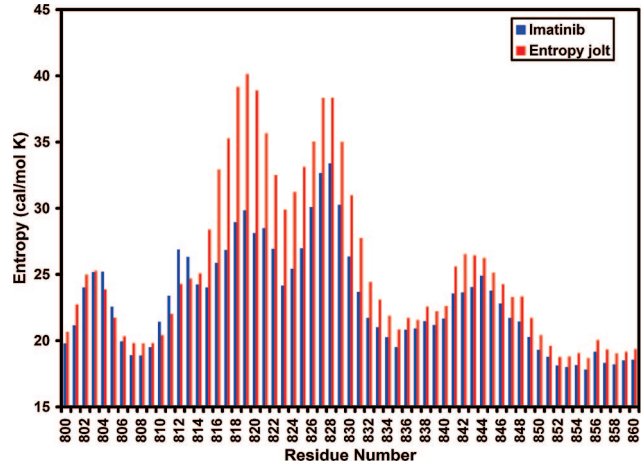

Figure 7. Entropic contribution (cal/mol K, 1 cal/mol *K* = 1 eu) as a function of the C-Kit residue number in the activation loop (residues 804 to 837) of the complex between imatinib (blue) or the entropy-boosting prototype (red) and the D816V mutant C-Kit kinase.

The prototype also inhibits the wild-type form of the C-Kit kinase with a binding free energy (ΔG_{bind}) of −18.2 kcal/mol (energetic contribution:, −57.25 kcal/mol; entropic contribution ($-T\Delta S$), 39.02 kcal/mol). It is more effective toward the wild-type kinase than imatinib, due to the expected entropy increase (3553 and 3537 eu, respectively). However, the entropic boost promoted by our prototype in the mutant is greater than in the wild-type (3582 and 3553

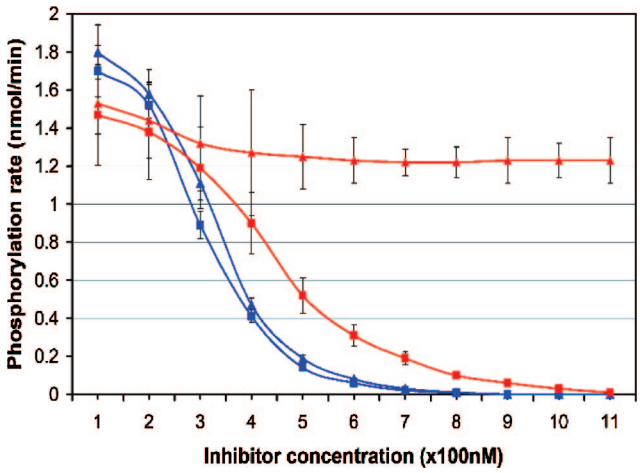

Figure 8. Downstream phosphorylation rates from spectrophotometric kinetic assay of active C-Kit kinase (blue) and active imatinib-resistant D816V mutant (red). Both kinases are inhibited by our entropy-boosting prototype (squares), while only the wild-type C-Kit is significantly inhibited by imatinib (triangles). The error bars represent dispersion over 5 runs for each kinetic assay, consisting of 11 measurements of maximum phosphorylation rate at 100 nM intervals in increasing inhibitor concentration (Materials and Methods).

eu, respectively) since the activation loop of the mutant is already destabilized in the unbound state with increased conformational flexibility. Thus, more disordered regions are prone to greater entropic boosts.

The spectrophotometric kinetic assays (Figure 8),[7] which measure the downstream phosphorylation rates of active wild-type and D816V mutant kinases as the inhibitor concentration is increased, confirmed the dual affinity of the prototype: *our entropy-boosting ligand is a nanomolar inhibitor* ($K_d \approx 47 \pm 11$ nM) *of the imatinib-resistant D816V mutant, as well as of the wild-type kinase* ($K_d \approx 22 \pm 7$ nM). The efficacy of the prototype was contrasted with the lack of activity of imatinib for the D816V mutant ($K_d \approx 12 \pm 2$ μM), reflected in a 250 times higher affinity for the imatinib-resistant kinase. However, imatinib is a nM inhibitor ($K_d \approx 21 \pm 5$ nM) of the wild-type C-Kit kinase, justifiably becoming a therapeutic agent for treating GIST tumors.[16,17] In all cases, the Michaelis–Menten scheme with ATP-competitive inhibition and saturating substrate concentration yield accurate fits. The standard deviations reported for the K_d values arise from fluctuations in initial enzyme concentration, generating dispersion in the phosphorylation rates, pronounced at low inhibitor concentration (since $K_m(\text{app}) \ll [\text{ATP}]$).

To test the selectivity of the entropy-boosting inhibitor, a high-throughput screening of its affinity pattern was performed (Ambit Biosciences, San Diego, CA) against a bacteriophage library displaying 240 human kinases (Figure 9), using imatinib screening as control.[21] The results shown in Figure 9 confirm the dual activity of the prototype on both wild-type and mutant C-Kit kinase and show an increased specificity compared with imatinib. Both drugs inhibit C-Kit

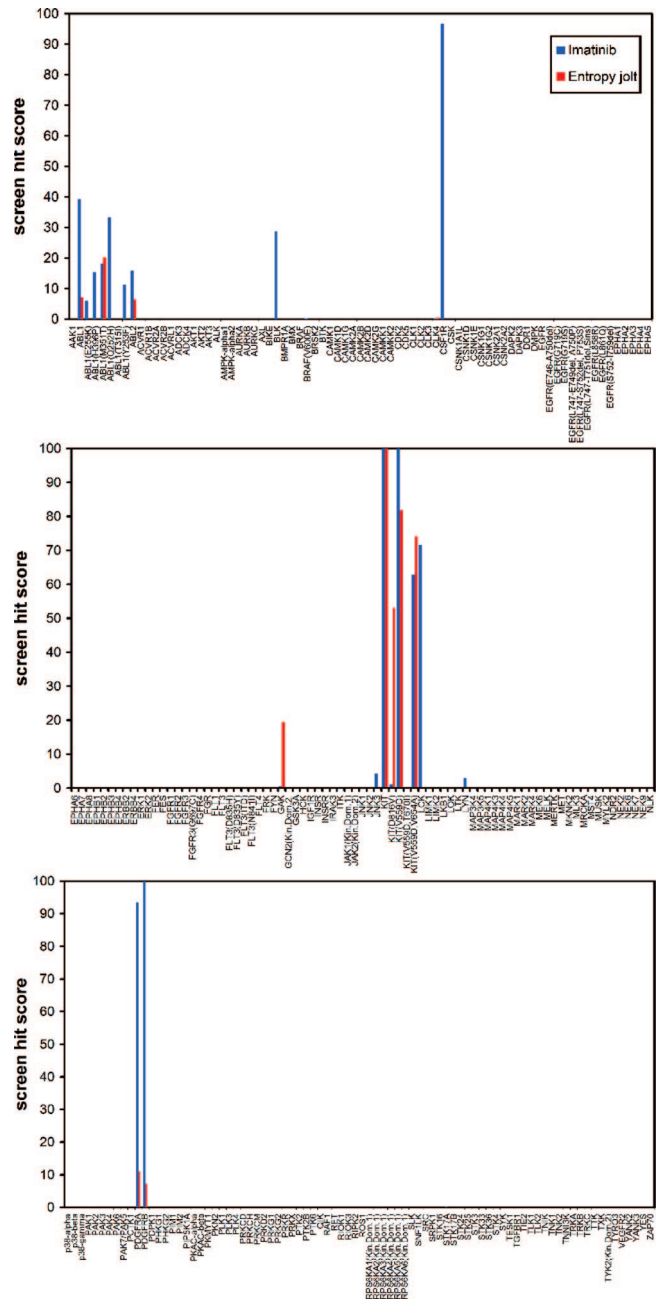

Figure 9. High-throughput screening of the entropy-boosting prototype (red) and imatinib (blue, control) over 240 human kinases displayed in a T7-bacteriophagelibrary (Ambit Biosciences, Methods). Hit values are reported as percentage bound kinase.

V559D mutations, since this residue belongs to the juxtamembrane domain of the kinase, far away from the inhibitor's binding pocket. However, neither imatinib nor the prototype inhibit the T670I mutation, since T670 is the conserved gate-keeper involved in inhibitor binding, and a mutation to a bulky isoleucine will hamper ligand association. Our entropy-boosting inhibitor is much more specific than the parental compound, since its affinity for the Bcr-Abl kinase is reduced by more than 75%. Moreover, it has no affinity toward LCK and a reduced activity for PDGFR, the other reported imatinib targets.[21] Nevertheless, the prototype

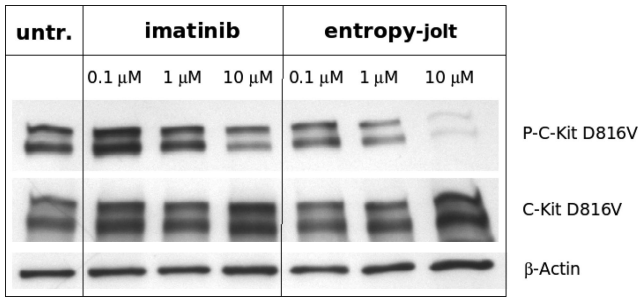

Figure 10. Western blot assay of murine Ba/F3 cells untreated, treated with our entropy-boosting prototype and with imatinib at different inhibitor concentrations (Materials and Methods). The upper band pair corresponds to the phosphorylated D816V mutant kinase, the intermediate bands, to the total C-Kit D816V kinase, and the lower is the β-Actin control.

shows some activity toward the Cyclin G-associated kinase (GAK). GAK is a serine/threonine kinase that features high homology outside its kinase domain with auxilin.[35] GAK is known to assist in uncoating clathrin-coated vesicles and has been reported to phosphorylate the μ2 subunit of adaptor protein (AP)2.[35] However, the effect of specifically inhibiting the GAK kinase is not completely understood, since mammalian cells also have the AAK1 kinase that performs the same function.[35]

The Western blot assays performed on Ba/F3 cells that express the D816V drug-resistant mutation (Figure 10) provided a characterization of the inhibitory activity of the prototype on kinase autophosphorylation. Densitometry revealed 90% inhibition of the D816V mutant by the prototype in comparison with only 22% inhibition of imatinib at 10 μM bulk concentration in Ba/F3 cells. Thus, the entropy-boosting modification of imatinib significantly enhances the inhibitory impact on autophosphorylation of the imatinib-resistant variant over the levels achieved by the parental compound.

(35) Lee, D.; Zhao, X.; Zhang, F.; Eisenberg, E.; Greene, L. E. Depletion of GAK/auxilin 2 inhibits receptor-mediated endocytosis and recruitment of both clathrin and clathrin adaptors. *J. Cell Sci.* **2005**, *118*, 4311–4321.

Conclusion

In this work we proposed and validated a drug-design strategy aimed at increasing the *entropy content* of floppy targets upon complexation as a means to enhance the drug affinity. Thus, we introduce the design concept of disorder-inducing drug ligand. The reported research addresses paradoxes in high-affinity protein–ligand complexation and identifies the foundational steps to launch a drug-design strategy based on controlled induced disorder. As proof of concept, we rationally developed a modification of imatinib that inhibits the D816V imatinib-resistant mutant C-Kit kinase, by promoting an entropy boost on the activation loop. The inhibitory and selective impact of our prototype was corroborated through *in vitro* kinetic assays, phage-display kinase screening and Western blots, validating our entropy-enhancing approach to drug design. From a structural biology perspective, these studies are likely to herald a paradigm shift as they mark a departure from the *order-upon-binding* scenario.

Acknowledgment. This research is supported by NIH (R01-GM072614), NSF (EIA-0216467), the John and Ann Doerr Fund for Computational Biomedicine, an unrestricted grant from Eli Lilly and the Rice Computational Research Cluster funded by NSF under Grant CNS-0421109. The authors thank Drs. Harry Harlow and Chen Su (Eli Lilly) for their valuable input.

Supporting Information Available: Molecular dynamic simulations details, total synthesis and spectroscopic characterization of the prototype, kinetic and Western blot assay details. This information is available free of charge via the Internet at http://pubs.acs.org.

MP700148H